J Mater Sci (2007) 42:9227–9233
DOI 10.1007/s10853-007-1908-z

On the feasibility of synthesizing complex perovskite ferroelectric ceramics via a B-site oxide mixing route

Bijun Fang · Renbing Sun · Yuejin Shan · Keitaro Tezuka · Hideo Imoto

Received: 5 March 2007 / Accepted: 31 May 2007 / Published online: 27 July 2007

Abstract Several relaxor-based complex perovskite ferroelectric ceramics were synthesized by conventional solid-state reaction method via different routes, i.e., the B-site oxide mixing route, the straight calcination method and the columbite/wolframite precursor method. Structure analysis and physical properties measurements prove that the B-site oxide mixing route is efficient and feasible in the synthesizing of complex perovskite ferroelectrics since such a technique is superior in suppressing pyrochlore phases, stabilizing the perovskite structure, and improving the amount of perovskite phase as compared to the straight calcination method and the columbite/wolframite precursor method. The dielectric properties are improved correspondingly, namely exhibiting the largest value of dielectric maximum, the sharpest dielectric response peaks and the least frequency dispersion of dielectric properties in the ferroelectric ceramics prepared via the B-site oxide mixing route, which is considered as correlating with the amount of pyrochlore phases, ceramic density, grain size, and microstructure morphology of the ceramics synthesized.

Introduction

Relaxor-based ferroelectrics have attracted considerable research attention due to their high and nearly temperature-insensitive dielectric constant and excellent piezoelectric properties as compared to normal ferroelectrics, which make them useful in multilayer capacitor, transducer and actuator applications [1–3]. Ferroelectric relaxors usually do not show sharp anomalies in the curves of dielectric response to temperature, and the dielectric behavior is characterized by broad and frequency-dispersive dielectric peaks [4–6]. The main structural feature of relaxors is the random occupation of the equivalent crystallographic positions by different heterovalent cations, which destructs the normal ferroelectric phase transition and makes the dependence of dielectric permittivity on electric field similar to that of magnetic permeability on magnetic field of disordered ferromagnetic materials [7]. The relaxor behavior, such as frequency dependence of the dielectric anomaly, and the presence of polar nanoregions (PNR) persisting hundreds of Kelvins above the temperature of dielectric maximum (T_m), is usually attributed to the polar clusters and/or the nanoscopic inhomogeneity induced by short-range occupational ordering on one or more symmetrical crystallographic positions of the perovskite structure [2, 5, 6].

A major disadvantage of ferroelectric relaxors is that they are very sensitive to processing varieties and difficult to synthesize reproducibly. Recently, great advances have been developed in relaxor-based single crystal piezoelectrics, such as $(1-x)Pb(Mg_{1/3}Nb_{2/3})O_3-xPT$ (PMNT) and $(1-x)Pb(Zn_{1/3}Nb_{2/3})O_3-xPT$ (PZNT). These materials exhibit ultrahigh electromechanical coupling factors, piezoelectric coefficients and strain level in single crystalline form, which implement potential benefits in terms of

B. Fang (✉) · R. Sun
Department of Materials Science and Engineering, Jiangsu Polytechnic University, Changzhou, Jiangsu 213164, China
e-mail: fangbj@sohu.com

Y. Shan · K. Tezuka · H. Imoto
Department of Applied Chemistry, Faculty of Engineering, Utsunomiya University, 7-1-2 Yoto, Utsunomiya 321-8585, Japan

Y. Shan
e-mail: shan@cc.utsunomiya-u.ac.jp

increased bandwidth, sensitivity and source levels [8, 9]. However, the growth of single crystals is not yet satisfactory; unacceptable high crystal growth cost accompanied by poor reproducibility of crystals as-grown, which cannot meet the abundant demands of commercial devices for large-size high-quality piezocrystals [10, 11]. Ferroelectric relaxors in polycrystalline ceramic form deserve major fields in dielectric/piezoelectric applications due to the relatively low production cost, good reproducible high-yield, and versatile properties which can meet the requirements of different commercial applications through tailoring the compositions of ferroelectrics fabricated [12, 13].

$Pb(Fe_{1/2}Nb_{1/2})O_3$ (PFN), $Pb(Sc_{1/2}Nb_{1/2})O_3$ (PSN), $Pb(Ni_{1/3}Nb_{2/3})O_3$ (PNN), and $Pb(Zn_{1/3}Nb_{2/3})O_3$ (PZN) with complex perovskite structure have been widely used in capacitor industry and related commercial fields [14–17]. PFN exhibits a large dielectric constant and low-temperature sintering capability, whereas it does not exhibit apparent frequency dispersion of T_m although PFN is a compositionally disordered ferroelectric relaxor. PSN is a typical relaxor and the degree of ordering of the B-site of the perovskite structure can be controlled by thermal treatment. PNN is also a relaxor-type ferroelectric and shares the same perovskite structure with PZN [14–17]. However, perovskite ferroelectrics are extremely difficult to fabricate/process reproducibly without the appearance of stable pyrochlore phases, which often deteriorates the dielectric properties. Swartz and Shrout devised a columbite precursor method to synthesize stoichiometric perovskite $Pb(Mg_{1/3}Nb_{2/3})O_3$ (PMN), where the intermediate reaction of formation of pyrochlore phases was bypassed, which results in the stabilization of perovskite structure as compared to the straight calcination method [18]. Orita et al. developed this technique to a B-site oxide mixing route, where all oxides of the B-site of the perovskite structure were mixed and calcined simultaneously instead of preparing different columbite/wolframite precursors separately. Such modification exhibits superior behavior in suppressing pyrochlore phases as compared to the columbite/wolframite precursor method, which can be attributed to the intermediate compounds formed during the calcination of the B-site oxides minimizing the preferential reaction of Nb_2O_5 with PbO to form stable pyrochlore phases [16, 19]. Recently, Liou et al. proposed a simplified columbite/wolframite route and a reaction-sintering process to synthesize relaxor ferroelectric ceramics, where repeated pulverization and calcination were omitted, which further simplifies the preparation of pyrochlore-free relaxor ferroelectrics [20–22].

In this article, the perovskite phase formation and physical properties of several ferroelectrics based on PFN, PSN, PNN, and PZN have been investigated. The B-site oxide mixing route has been adopted to synthesize these ferroelectrics, where two alternate methods, i.e., the direct solid-state reaction method and the columbite/wolframite precursor method, have been tried and their influences on phase formation and physical properties have been discussed. The efficiency and feasibility of the B-site oxide mixing route in synthesizing complex perovskite ferroelectric ceramics have been proven again since these ferroelectrics synthesized exhibit enhanced stabilization of perovskite structure accompanied by improved dielectric properties as compared to those fabricated by the straight calcination route and the columbite/wolframite precursor method.

Experimental procedure

Several perovskite relaxors: xPFN–yPZ–(1–x–y)PT (PZ and PT stand for $PbZrO_3$ and $PbTiO_3$, respectively), xPFN–yPSN–(1–x–y)PT and xPNN–yPZN–(1–x–y)PT were prepared by conventional ceramic processing via the B-site oxide mixing route. The B-site oxide mixing route technique is a modified columbite/wolframite precursor method, where all oxides of the B-site positions of the perovskite structure were mixed and pre-calcined together simultaneously instead of preparing different columbite/wolframite precursors separately. High-purity oxides, PbO (>99.9%), Fe_2O_3 (>99.99%), Nb_2O_5 (>99.9%), ZrO_2 (>99.9%), TiO_2 (>99.9%), Sc_2O_3 (>99.9%), NiO (99.9%), and ZnO (>99.95%), were used as raw materials. To maintain stoichiometric the raw materials were dried before weighing and the synthesized B-site precursors were weighed and introduced into the batch calculation. The B-site oxides (according to the formula composition) were ground and pre-calcined at different conditions (shown in Table 1). No free Nb_2O_5 retains in the obtained B-site precursors (JCPDS files 27-1311 and 37-1468) confirmed by X-ray diffraction measurement (XRD, Rigaku RINT-2200VS Diffractometer). Stoichiometric PbO was added to the synthesized B-site precursors, respectively, and the mixed powders were calcined at different conditions (Table 1). The amount of perovskite phases was analyzed by XRD measurement. The calcined powders were then isostatically pressed into pellets at a pressure of 400 kgf/cm^2 with the addition of 1 wt.% polyvinyl alcohol (PVA) binder and sintered at different conditions (Table 1). The disk pellets were buried under an equiweight mixed raw oxides (with the same composition) in a covered crucible to minimize the volatilization of lead during sintering.

The straight calcination route and the columbite/wolframite precursor method were also used to investigate the influences of synthesis methods on perovskite phase formation and physical properties. The B-site oxide mixing route exhibit superior behavior in terms of suppressing

Table 1 Synthesis conditions and percentage of perovskite phase of calcined and sintered ferroelectrics prepared by three methods [7, 14–17, 20]

Synthesis conditions	B-site oxide mixing route		Columbite/Wolframite precursor method		Straight calcination method	
PFN-PZ-PT	B-oxides 1000	4 h	$FeNbO_4$ 1000	4h		
	Calcine 950	2 h	Calcine 950	2 h	Calcine 950	2 h
	Sinter 1175	2 h	Sinter 1175	2 h	Sinter 1175	2 h
PFSN-PT	B-oxides 1200	3 h	$ScNbO_4$ 1200	3 h		
	Calcine 900	2 h	$FeNbO_4$ 1000	4 h	Calcine 900	2 h
	Sinter 1160	2 h	Calcine 900	2 h	Sinter 1160	2 h
			Sinter 1160	2 h		
PNN-PZN-PT	B-oxides 1000	4 h	$NiNb_2O_6$ 1000	4 h		
	Calcine 925	2 h	$ZnNb_2O_6$ 1000	4 h	Calcine 925	2 h
	Sinter 1185	2 h	Calcine 925	2 h	Sinter 1185	2 h
			Sinter 1185	2 h		
Percentage of perovskite phase	B-site oxide mixing route		Columbite/Wolframite precursor method		Straight calcination method	
	Calcined	Sintered	Calcined	Sintered	Calcined	Sintered
PFN20-PZ45-PT35	97.5	100	96.2	98.5	89.4	90.2
PFN40-PZ34-PT26	97.9	100	98.2	98.6	92.7	91.4
PFN60-PZ22-PT18	100	100	98.8	100	94.9	96.2
PFSN	100	100	96.2	100	92.1	100
PFSN80-PT20	100	100	94.8	100	91.9	100
PNN40-PZN10-PT50	97.0	97.6	95.8	94.6	86.1	88.8
PNN64-PZN10-PT26	92.6	94.5	89.7	89.8	82.7	68.5

PFSN stands for $Pb(Fe_{1/4}Sc_{1/4}Nb_{1/2})O_3$. The compositions are designed in molar percentage

pyrochlore phases, stabilizing perovskite structure, and improving the amount of perovskite phase.

In all of the above methods no excess of PbO was added and the calcination and sintering were carried out in closed aluminum crucibles. The structure of the calcined and sintered samples were analyzed by XRD measurement and the perovskite phase formation can be calculated using an approximate method:

$$\%\ \text{perovskite} = \frac{I_{\text{perov}} \times 100}{I_{\text{perov}} + I_{\text{Pyro}}} \tag{1}$$

where the concentration of perovskite and pyrochlore phases was determined by the relative intensity of the (110) perovskite peak (I_{perov}) and the (222) pyrochlore peak (I_{pyro}) [16]. For electrical characterization, silver paste was coated on both surfaces of the well-polished pellets and fired at 650 °C for 15 min to provide robust electrodes. Detailed measurement procedures were described elsewhere [23, 24].

Results and discussion

The synthesis conditions and the amount of perovskite phase estimated from XRD patterns of various compositions are shown in Table 1. For the compounds investigated, the B-site oxide mixing route exhibits increased stabilization of perovskite structure, especially for the PFN- and PSN-containing ferroelectrics, which can be attributed to their stable perovskite structure. Pure perovskite structure can be obtained after calcining, and the perovskite phase stabilizes further upon sintering. For the PZN-containing system, the B-site oxide mixing route also fails to give pure perovskite structure and $Pb_3Nb_4O_{13}$-type pyrochlore phases appear in all three methods with different content. The decreased amount of perovskite phase in the PZN-containing compounds can be ascribed to the metastability of perovskite PZN, which decomposes easily into pyrochlore phases during sintering. Such a tendency of the formation of perovskite phase is consistent with the relatively easy of the fabrication of perovskite ferroelectrics, which is considered as correlating with tolerance factor, electronegativity difference, and bonding and structure parameters [1, 18, 19].

The success of the B-site oxide mixing route in suppressing pyrochlore phases can be attributed to the intermediate compounds formed after pre-calcination. The $FeNbO_4$, $ScNbO_4$, $NiNb_2O_6$, and $ZnNb_2O_6$ precursors in the columbite/wolframite precursor method give well-crystallized XRD patterns corresponding to JCPDS files 16-358, 24-1013, 32-0694, and 37-1371, respectively. As a comparison, the diffraction peaks of the B-site oxide mixing route precursors are broad and the background of XRD patterns is noisy, which are similar to and between above patterns, accounting for the poor crystallizability and the crystalline phases being some kind of solid solutions between above precursors. However, no any trace of Nb_2O_5 (JCPDS files 27-1311 and 37-1468) retains in the B-site oxide mixing route precursors. This minimizes the preferential reaction of Nb_2O_5 with PbO to form stable pyrochlore phase and interprets the superior behavior of this technique as compared to the columbite/wolframite precursor method [19]. Figure 1 shows the XRD patterns of intermediate precursors and PFSN ceramics prepared by different methods as example. Detailed XRD patterns and the influence of synthesis methods on perovskite structure of other systems were discussed elsewhere [23, 24].

Optimized dielectric properties of several lead-based complex perovskites obtained via the B-site oxide mixing route are shown in Fig. 2. The dielectric anomalies appearing at different temperatures are called the “critical slowing down” and are characteristic of ferroelectric systems near the ferroelectric-paraelectric (FE-PE) phase transition points. With the temperature approaching T_m, ferroelectric polar clusters and/or long-range ferroelectric ordering develop, which contribute largely to the dielectric response, leading to the dielectric anomalies [25]. In the PFN-PZ-PT system, with the increase of the concentration of PFN, the dielectric peaks become broader and exhibit frequency dispersive character. In the PNN-PZN-PT system, with the increase of the concentration of PT, the FE-PE transition changes from a diffused ferroelectric transition of relaxor ferroelectrics to a first-order ferroelectric transition of normal ferroelectrics. The abnormal increase of dielectric constant in the paraelectric region in the iron-containing ferroelectrics, which exhibits strong frequency dependence accompanied by a large increase of dielectric loss, is considered as correlating with the partial reduction of Fe^{3+} to Fe^{2+} ions during sintering. The co-existence of Fe^{3+} and Fe^{2+} cations on equivalent crystallographic sites affords finite hopping/jump type of conduction mechanism, which is highly sensitive to sintering temperature and tends to take effects at lower frequencies [26].

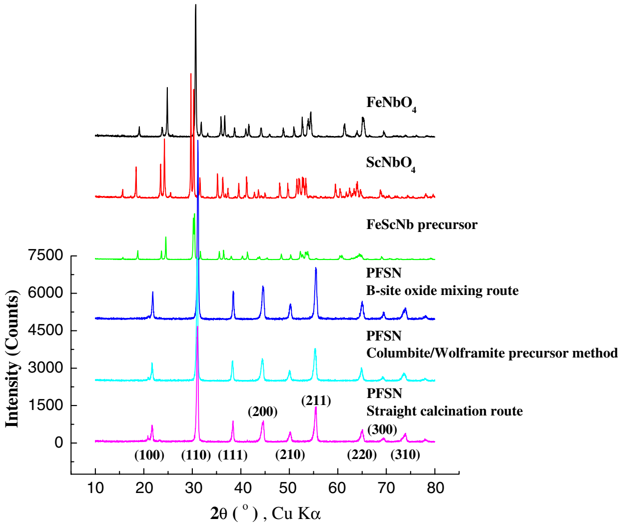

Fig. 1 XRD patterns of the PFSN ceramics prepared by different methods. XRD patterns of some precursors are also shown here for comparison

The dielectric behavior above T_m of the ferroelectrics exhibiting normal ferroelectric phase transition can be described by the Curie-Weiss law:

$$\varepsilon = \frac{C}{T - T_0} \tag{2}$$

where C is the Curie-Weiss constant and T_0 is the Curie-Weiss temperature. Figure 3 shows the temperature dependence of the reciprocal dielectric constant of some “normal” ferroelectrics, where the solid lines are linear fitting of the dielectric properties according to the Curie-Weiss law. $PbTiO_3$ exhibits special function to change the relaxor ferroelectric behavior to normal ferroelectric behavior when it was added into relaxors to form solid solutions. The dielectric behavior deviates greatly from the Curie-Weiss law at elevated temperatures in the iron-containing ferroelectrics, which is believed relating to the thermally activated hole conduction induced by the partial reduction of Fe^{3+} to Fe^{2+} ions during sintering.

The room-temperature dielectric properties of several relaxor-based ferroelectric ceramics synthesized by three methods are given in Table 2. The samples prepared via the B-site oxide mixing route exhibit very high values of dielectric constant (ε). Normally, dielectric constant of the samples prepared by the straight calcination method is the lowest since the ferroelectric ceramics obtained contain pyrochlore phases, indicating that the formation of pyrochlore phases significantly decreases dielectric constant and increases dielectric loss (tanδ). In PFSN system ferroelectrics, the ceramics prepared by the straight calcination method exhibit the largest dielectric constant, which is considered as correlating with the relatively high dielectric loss, ceramic density, and microstructure (especially grain size) [15, 23, 24].

Detailed dielectric properties are shown in Fig. 4 using some ferroelectric ceramics as example. Although PFSN obtained is of pure perovskite phase prepared by all three methods, the ceramics synthesized via the B-site oxide mixing route exhibit the largest values of dielectric maximum (ε_m) and the sharpest dielectric response peaks. ε_m of the samples obtained by the straight calcination method is

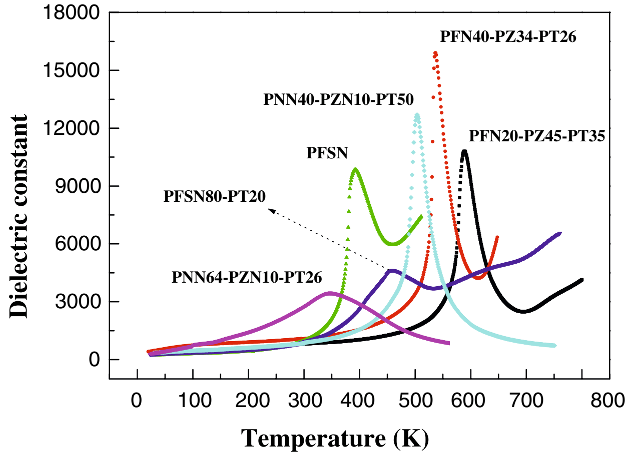

Fig. 2 Optimized dielectric properties of several perovskite relaxor-based ferroelectric ceramics synthesized via the B-site oxide mixing route measured at 100 kHz upon heating

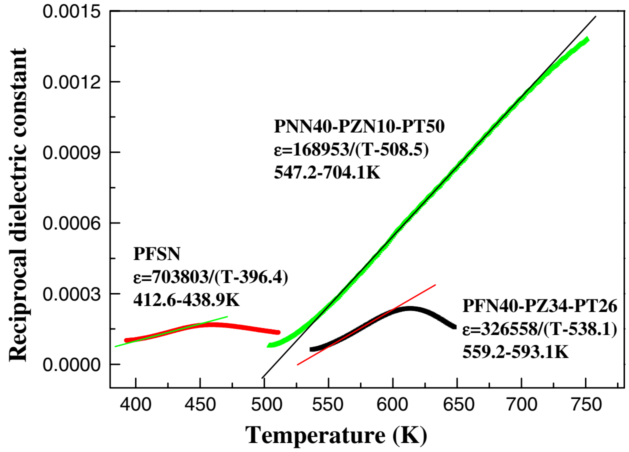

Fig. 3 Temperature dependence of the reciprocal dielectric constant of several "normal" ferroelectrics obtained via the B-site oxide mixing route measured at 100 kHz upon heating. The solid lines are linear fitting of the dielectric behavior above T_m according to the Curie-Weiss law. The fitting parameters and the temperature range where the Curie-Weiss law takes effect are shown in the plot

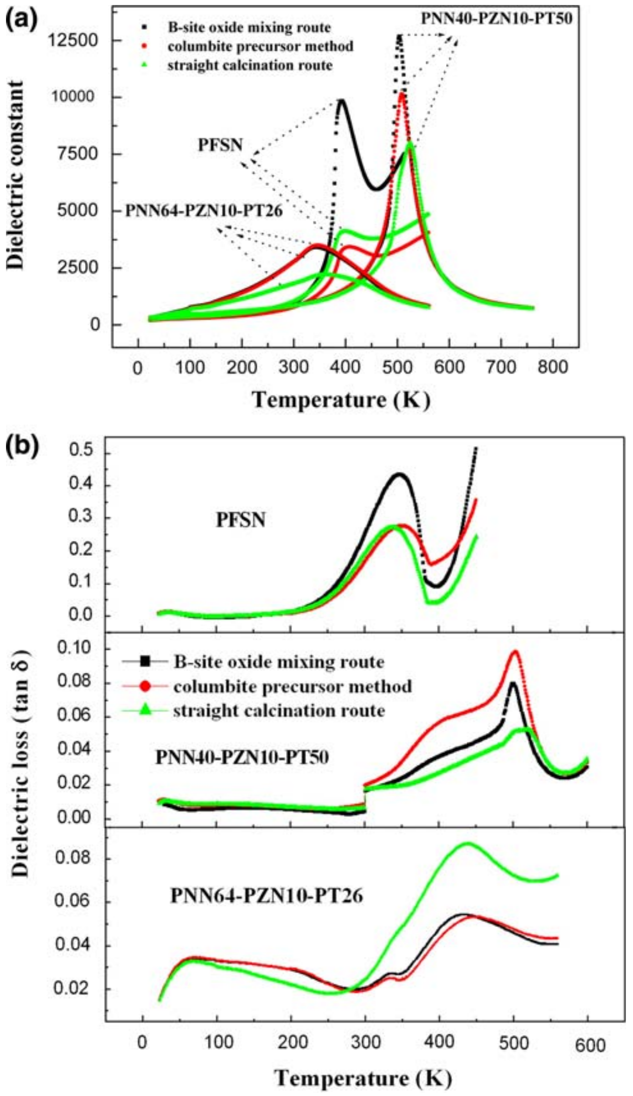

Fig. 4 Temperature dependence of the dielectric constant (**a**) and loss tangent (**b**) of several relaxor-based ferroelectric ceramics prepared by three methods measured at 100 kHz upon heating

Table 2 Room-temperature dielectric constant and loss tangent of several relaxor-based ferroelectric ceramics prepared by three methods measured at 100 kHz

Ferroelectric ceramics	B-site oxide mixing route		Columbite/Wolframite precursor method		Straight calcination method	
	Dielectric constant	Dielectric loss	Dielectric constant	Dielectric loss	Dielectric constant	Dielectric loss
PFSN	977.5	0.2455	783.1	0.1635	1,032	0.1915
PFSN80-PT20	952.4	0.06907	929.1	0.08298	9,78.8	0.165
PNN40-PZN10-PT50	842.8	0.00422	855.2	0.00856	819.0	0.00639
PNN56-PZN10-PT34	2056	0.01189	2,047	0.00941	1,667	0.00795
PNN64-PZN10-PT26	2,754	0.02054	2,768	0.01935	1,808	0.02462

slightly larger than that by the columbite/wolframite precursor method, which is considered as correlating with the slightly larger dielectric loss. Temperature of the dielectric maximum (T_m) exhibits almost independence on preparation methods. In the PNN-PZN-PT system, the appearance of pyrochlore phases deteriorates dielectric properties. Normally, the more the pyrochlore phases have, the worse the dielectric properties would be. Furthermore, with the increase of the amount of pyrochlore phases, the values of dielectric constant decrease accompanied by the broadening of the dielectric response peaks. However, dielectric loss is lower for the ceramics obtained by the straight calcination route than that by the columbite/wolframite precursor method, which in turn are lower than that via the B-site oxide mixing route in some compositions. The dielectric loss in the PFSN system and other iron-containing ferroelectrics is relatively large (especially with large concentration of iron) accompanied by strong frequency dispersion of dielectric response, which is usually observed in lossy ferroelectrics [26, 27]. Such anomalous phenomena are considered as relating to the nature of the iron-containing ferroelectrics, i.e., the existence of residual semi-conductive $FeNbO_4$ and/or $ScNbO_4$ and the partial reduction of Fe^{3+} to Fe^{2+} ions during sintering, which leads to finite hopping/jump type of conduction mechanism. Such thermally activated hole conduction can be reduced significantly by the addition of small amounts of manganese oxide or lithium carbonate [23, 24, 28].

Microstructure morphology of the relaxor-based ferroelectrics synthesized by three methods is observed by SEM (HITACHI S-4500 Scanning Electron Microscope) using PNN64-PZN10-PT26 ceramics as example (Fig. 5). SEM photograph of the PNN64-PZN10-PT26 ceramics prepared via the B-site oxide mixing route exhibits rather homogeneous microstructure accompanied by large quantities of fine granules, major in grain junctures and minor in grain surface, which are considered as being the $Pb_3Nb_4O_{13}$-type pyrochlore phases [The content of the pyrochlore phases is too small to give undoubted structure by XRD measurement and the energy-dispersive X-ray analyzer (HORIBA EMAX-5770W X-ray Microanalyzer) attached to the SEM equipment can only give possible chemical composition. Therefore, $Pb_3Nb_4O_{13}$-type pyrochlore phases are used to indicate the impurities.]. Liquid-phase sintering mechanism may take partial effect in the densification of the PNN64-PZN10-PT26 ceramics due to the round grain morphology. As a comparison, a lot of rodlike granules aggregate in the matrix of the irregular PNN64-PZN10-PT26 grains obtained by the columbite/wolframite precursor method; and the grains of the PNN64-PZN10-PT26 ceramics fabricated by the straight calcination method exhibit octahedral or other polyhedral morphology. Exaggerated growth of abnormal grains with polyhedral shape is all found in the PNN64-PZN10-PT26 ceramics prepared by three methods, and the quantity is especially large in the straight calcination method. Such character of the microstructure morphology (especially the densification of ceramics and the grain size) of the PNN64-PZN10-PT26 ceramics prepared by different methods are considered as exerting important influence on the dielectric properties of the ceramics obtained.

Conclusions

Relaxor-based complex perovskite ferroelectrics (PFN-, PSN-, and PNN-based ferroelectric ceramics) were successfully synthesized by conventional solid-state reaction method via the B-site oxide mixing route. Such a technique exhibits superior behavior in suppressing pyrochlore phases, stabilizing perovskite structure, and improving the amount of perovskite phase. The ferroelectric ceramics obtained exhibit superior dielectric properties as compared to the equi-composition samples prepared by the straight calcination method and the columbite/wolframite precursor method, accompanied by improved dielectric loss performance and frequency dispersion character of the dielectric response. The amount of pyrochlore phases, the density of ceramics, the grain size, and the microstructure morphology are major factors that influence the dielectric properties of relaxor-based ferroelectric ceramics, which provide feasibility to tailor dielectric properties through modifying composition, the degrees of ordering of the B-site of the perovskite structure and manufacture technique.

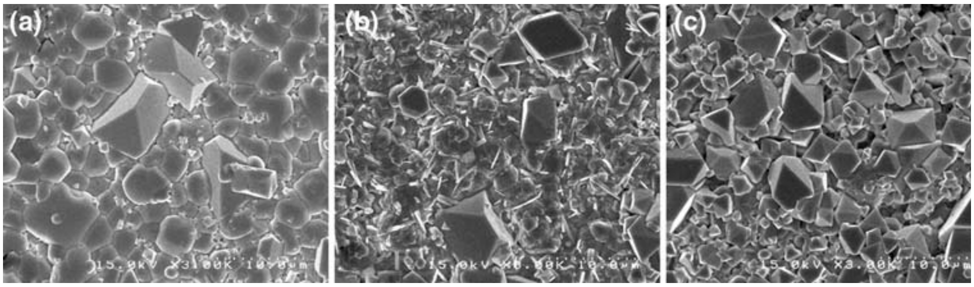

Fig. 5 SEM photographs of the PNN64-PZN10-PT26 ceramics prepared by different methods. (**a**) B-site oxide mixing route; (**b**) Columbite/Wolframite precursor method; (**c**) Straight calcination method

Acknowledgments The authors thank the Satellite Venture Business Laboratory of Utsunomiya University, Japan, and Jiangsu Polytechnic University, China, for financial support. One of the authors also thanks the Scientific Research Foundation for the Returned Overseas Chinese Scholars, State Education Ministry for financial support.

References

1. Shrout TR, Halliyal A (1987) Am Ceram Soc Bull 66:704
2. Viehland D, Jang SJ, Cross LE, Wuttig M (1990) J Appl Phys 68:2916
3. Fang B-J, Shan Y-J, Xu H-Q, Luo H-S, Yin Z-W (2004) Adv Funct Mater 2:169
4. Bokov AA, Bing Y-H, Chen W, Ye Z-G, Bogatina SA, Raevski IP, Raevskaya SI, Sahkar EV (2003) Phys Rev B 68:052102
5. Noheda B (2002) Curr Opin Solid State Mater Sci 6:27
6. Ye Z-G (2002) Curr Opin Solid State Mater Sci 6:35
7. Haumont R, Dkhil B, Kiat JM, Al-Barakaty A, Dammak H, Bellaiche L (2003) Phys Rev B 68:014114
8. Saitoh S, Kobayashi T, Harada K, Shimanuki S, Yamashita Y (1998) IEEE Trans Ultrason Ferroelectr Freq Control 45:1071
9. Park SE, Shrout TR (1997) IEEE Trans Ultrason Ferroelectr Freq Control 44:1140
10. Fang B-J, Luo H, Xu H, He T, Yin Z (2001) Jpn J Appl Phys Part 2 40:L1377
11. Luo H, Xu G, Xu H, Wang P, Yin Z (2000) Jpn J Appl Phys Part 1 39:5581
12. Kanai H, Furukawa O, Nakamura S, Yamashita Y (1993) J Am Ceram Soc 76:451
13. Lee D-H, Kim N-K (1998) Mater Lett 34:299
14. Ichinose N, Kato N (1994) Jpn J Appl Phys Part 1 33:5423
15. Ichinose N, Natsume S, Yamashita Y (1999) J Eur Ceram Soc 19:1139
16. Rao RMV, Halliyal A, Umarji AM (1996) J Am Ceram Soc 79:257
17. Lei C, Chen K, Zhang X-W (2002) Mater Lett 54:8
18. Swartz SL, Shrout TR (1982) Mater Res Bull 17:1245
19. Orita M, Satoh H, Aizawa K, Ametani K (1992) Jpn. J Appl Phys Part 1 31:3261
20. Liou Y-C, Shih C-Y, Yu C-H (2002) Jpn J Appl Phys Part 1 41:3829
21. Liou Y-C, Tseng K-H (2003) Mater Res Bull 38:1351
22. Chen J-H, Liou Y-C (2004) Ceram Int 30:157
23. Fang B-J, Shan Y-J, Tezuka K, Imoto H (2005) J Mater Sci 40:6445, DOI: 10.1007/s10853-005-1711-7
24. Fang B-J, Shan Y-J, Tezuka K, Imoto H (2006) J Eur Ceram Soc 26:867
25. Kim B-G, Cho SM, Kim T-Y, Jang HM (2001) Phys Rev Lett 86:3404
26. Park KB, Yoon KH (1993) Ferroelectrics 145:195
27. Lee B-H, Min K-K, Kim N-K (2000) J Mater Sci 35:197, DOI: 10.1023/A: 1004773406645
28. Kassarjian MP, Newnham RE, Biggers JV (1985) Am Ceram Soc Bull 64:245